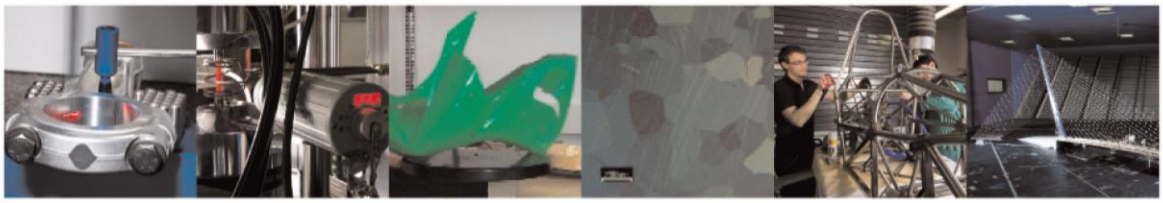

A path planning algorithm for industrial processes under velocity constraints with an application to additive manufacturing

Giberti, Hermes; Sbaglia, Luca; Urgo, Marcello

This is a post-peer-review, pre-copyedit version of an article published in JOURNAL OF MANUFACTURING SYSTEMS. The final authenticated version is available online at: http://dx.doi.org/10.1016/j.jmsy.2017.03.003

DIPARTIMENTO DI MECCANICA ■ POLITECNICO DI MILANO
via G. La Masa, 1 ■ 20156 Milano ■ EMAIL (PEC): pecmecc@cert.polimi.it
http://www.mecc.polimi.it
Rev. 0

A path planning algorithm for industrial processes under velocity constraints with an application to additive manufacturing

Hermes Giberti[a], Luca Sbaglia[b], Marcello Urgo[c]

[a] *Università degli Studi di Pavia, Dipartimento di Ingegneria Industriale e dell'Informazione, Via A. Ferrata 5, 27100 Pavia, Italy*
[b] *Università degli Studi di Parma, Industrial Engineering Department, Via delle Scienze 181/A, 43124 Parma, Italy*
[c] *Politecnico di Milano, Mechanical Department, via la Masa 1, 20156 Milano, Italy*

Abstract

In the execution of a wide class of industrial processes the use of robots with trajectories constrained by the velocity of the actuated parts (tools, end effectors, joints, etc.) often play a significant role. Focusing on systems for material deposition as are painting, gluing, aerosol spray but also today additive manufacturing techniques as FDM processes, it's possible to notice how a key parameter is the control of the material flow in accordance with the trajectory velocities of the actuated parts. In this paper we propose a path planning algorithm based on the use of Bézier curves aiming at guaranteeing a regulation on the velocity and, referring to additive manufacturing applications, an uniform distribution of the extruded material. The paper also presents a real application with a machine prototype in order to demonstrate the viability and performance of the approach and the impact on the actuators.

Keywords: path planning algorithm, Bézier curves, additive manufacturing, constant feed rate, constant extrusion rate,

Email addresses: `hermes.giberti@unipv.it` (Hermes Giberti), `luca.sbaglia@studenti.unipr.it` (Luca Sbaglia), `marcello.urgo@polimi.it` (Marcello Urgo)

1. Introduction and Problem Statement

Path planning is well known in robotics, aiming at defining the trajectory and movement of an end effector in the robot workspace. As robots are more and more used in the execution of a wide range of industrial processes, the importance of path planning, together with process planning, is considerably increased, to support the control of the process in terms of both motion and technological parameters. A popular field where this class of problems is additionally addressed is additive manufacturing (AM), due to the increasing adoption of this technology to process new shapes and materials.

The research presented in this article grounds on the need of jointly managing motion planning and process planning in the development of an innovative process technology together with the equipment to implement it. The need of coping with a wide set of limitation asked for the need of path planning respecting some specific constraints imposed by the process. Hence, we propose a path planning algorithm to ensure an uniform material distribution in a specific range of industrial processes, e.g., painting, gluing, aerosol spray and additive FDM processes. The addressed problem is tailored to extrusion processes where the extrusion rate cannot be controlled in an adequate way. The proposed path planning algorithm is grounds on Beziér curves to guarantee a proper control of the relative velocity between the end-effector and the part to process. Bézier curves are exploited for the generation of an interpolation of the ideal trajectory based on straight and parabolic segments. Regulating the parametric velocity along the trajectory, the approach allows to move a tool centre point (TCP), with regulated (constant) velocity during almost all the trajectory. Minimal oscillations in the velocity are unavoidable but the proposed approach is demonstrated to keep these fluctuations very low and, hence, negligible in most of the mentioned application fields. An extension of the approach towards the allowance of a given range of variability of the velocity is also outlined. Finally, the path planning approach is applied to an additive manufacturing machine prototype to demonstrate its applicability and performance.

2. Literature Review

Among AM techniques the ones based on the extrusion of material, as FDM, are the most studied in particularly after that the patent [1] about this technology is expired and so making spread this technique in the market. Roberson et al. [2] show the use of an FDM technique for new materials in the manufacture of electromechanical and electromagnetic applications, Volpato et al. [3] show an innovative piston-driven extrusion head that can extrude polypropylene granules into a filament and in previous works Giberti et al.[4],[5], [6] show several studies on a new 3D printing solution for metal parts based on a MIM technique. Other studies are focused on the optimization of these technique parameters, [7], or on the attempt to model particular characteristics of this process, [8][9]. Jiang et al.[10] show how much important is to obtain a uniform-distributed material thickness which is fundamental for the accuracy of this process. Without the control of this parameter these studies are affected by uncertainties which are not evaluable.

It must be taken into great consideration the deposition method and the tool path generation of the AM technique considered according to the different goals to be achieved. Kulkarni et al.[11] study the importance of the tool path planning on the resulting stiffness of the printed object. Jin et al.[12][13] propose a new path planning algorithm in order to minimize the building time of the part keeping at the same time a good surface accuracy. In order to face deposition problems, related to a new metal based AM technique, Mireles et al.[14] had to modify the toolpath commands of a pre-existent FDM machine.

Rishi [15] has shown how a different feed rate can be used to improve accuracy of the surface or the building time of the internal parts; instead for systems based on a constant feed rate in order to guarantee a uniform material deposition the Direction-Parallel Tool-Path (DP) technique can be used to achieve this goal. In literature are available some articles which propose DP deposition trajectories using a lines and parabolas approach, moving the end-tool with constant feed rate for almost the all trajectory. Thompson [16] shows constant

material flow trajectories for straight lines using a constant acceleration to link the velocity for two consecutive lines with different velocities: in this way is introduced an error on absolute velocity as bigger as smaller is the angle between the two consecutive lines leading to the necessity to change the material flow during the parabolic segments. Jin [17] suggests a straight lines and parabolas trajectory based entirely on the curvilinear abscissa velocity control. Defining two lines typologies (type I for lines which intersects the deposition profile, and type II for lines adjacent to the profile boundaries) a different absolute velocity is imposed on the two types: usually velocity I is doubler than velocity II and a constant acceleration profile is used to link the two lines on the curvilinear abscissa. The extruder motion profile is created taking into account the velocity variations of the control parameter. This strategy leads to limited accelerations on active joints during curved paths keeping a good printing velocity. In a different field of application as CNC machining the use of Bézier curves has been exploited in order to obtain continuity on the velocity and acceleration usually denied by the G-Code generated based on straight lines and the use of G1 commands[18].

3. Curve Parametrization

To define a trajectory in a cartesian space (XYZ) is necessary to define a parametric geometrical path, as defined by [19]:

$$\mathbf{p} = \mathbf{p}(u), \qquad u \in [u_{min}, u_{max}] \tag{1}$$

where $\mathbf{p}(u)$ is a continuous vectorial function(3x1) which describes the path inside the workspace as a function of the independent variable u. We take into account 3 Dofs, but we can extend the definition of $\mathbf{p}$ in order to include more Dofs.

The so defined vector function is controlled imposing a motion profile on parameter $u = u(t)$ which describes the tool trajectory along its path.

in particular:

$$\left|\dot{\tilde{\mathbf{p}}}(t)\right| = v_c = constant \tag{2}$$

where $\tilde{\mathbf{p}}(t) = (\mathbf{p} \circ u)(t)$, and for velocity and acceleration we derive the last equation.

It's not needed to analytical obtain function $u(t)$, its value $u(t_k) = u_k$ can be computed with a temporal discretization $t_k = kT_s$, with T_s sample time. We can obtain u_k with $k = 0, 1, 2, ...$, using a Taylor series with a second order approximation. Deriving respect to the time the following conditions are obtained:

$$\dot{u}(t) = \frac{v_c}{\left|\dfrac{d\mathbf{p}}{du}\right|} \qquad\qquad \ddot{u}(t) = -v_c^2 \frac{\dfrac{d\mathbf{p}^T}{du} \cdot \dfrac{d^2\mathbf{p}}{du^2}}{\left|\dfrac{d\mathbf{p}}{du}\right|^4} \tag{3}$$

considering a second order approximation the variable value u at time $(k+1)T_s$ can be determined as:

$$u_{k+1} = u_k + \frac{v_c T_s}{\left|\dfrac{d\mathbf{p}}{du}\right|_{u_k}} - \frac{(v_c T_s)^2}{2} \left[\frac{\dfrac{d\mathbf{p}^T}{du} \cdot \dfrac{d^2\mathbf{p}}{du^2}}{\left|\dfrac{d\mathbf{p}}{du}\right|^4} \right]_{u_k} \tag{4}$$

In order to achieve a constant velocity trajectory in the initial and final part of the path there is a non-zero acceleration. Considering a trapezoidal velocity the computing of u_{k+1} is modified as follow:

$$u_{k+1} = u_k + \frac{v_k T_s}{\left|\dfrac{d\mathbf{p}}{du}\right|_{u_k}} + \frac{T_s^2}{2} \left\{ \frac{a_k}{\left|\dfrac{d\mathbf{p}}{du}\right|_{u_k}} - v_k^2 \left[\frac{\dfrac{d\mathbf{p}^T}{du} \cdot \dfrac{d^2\mathbf{p}}{du^2}}{\left|\dfrac{d\mathbf{p}}{du}\right|^4} \right]_{u_k} \right\} \tag{5}$$

where $a_k = a(t_k)$ and $v_k = v(t_k)$ are respectively acceleration and velocity at instant $t_k = k \cdot T_s$.

To define a deposition trajectory which guarantees a constant feed rate of the tool in necessary to implement a parametric curve defined in the tool workspace.

In order to achieve this goal *Bézier curves*, are exploited to generate a parametric path made of straight lines and parabolas.

A *Bézier curve* of m degree is defined as:

$$\mathbf{b}(u) = \sum_{j=0}^{m} B_j^m(u)\mathbf{p}_j, \qquad 0 \leq u \leq 1 \tag{6}$$

where coefficients $\mathbf{p}_j$ are control points, and functions $B_j^M(u)$ are *Bernstein polynomials* defined as $B_j^m(u) = \binom{m}{j} u^j(1-u)^{m-j}$.

The Binomial coefficient, for $j = 0, 1, ..., m$, defines the rows of the *Pascal* triangle. A *Bézier curve* derivative respect to variable u of m degree is still a *Bézier curve* of degree $m-1$ defined as:

$$\frac{d\mathbf{b}(u)}{du} = m \sum_{i=0}^{m-1} B_i^{m-1}(u)(\mathbf{p}_{i+1} - \mathbf{p_i}) \tag{7}$$

4. Path planning with constant velocity using Bézier Curves

In this section, the path planning problem is addressed, subject to constant velocity along the path. The path planning approach uses straight lines and parabolas interpolation through *Bézier curves* of first and second degree. They are evaluated in the following way:

$$\begin{aligned} \mathbf{b}(u) &= (1-u)\mathbf{p}_{j-1}^u + u\mathbf{p}_j^e && \textit{line} \\ \mathbf{b}(u) &= (1-u)^2\mathbf{p}_j^e + 2u(1-u)\mathbf{p}_j + u^2\mathbf{p}_j^u && \textit{parabola} \end{aligned} \tag{8}$$

The complete trajectory is obtained merging a sequence of straight lines and parabolas whose parametrization is independent from each other in the range $u \in [0, 1]$. This method simplifies the definition of the equation for the trajectory, although the evaluation of the motion profile of parameter u becomes more complicated, as it will be shown later.

To provide an explanatory example, Fig.1 reports a set of control points $\mathbf{p}_j$ in the workspace. They are used to interpolate trajectory, linking straight lines

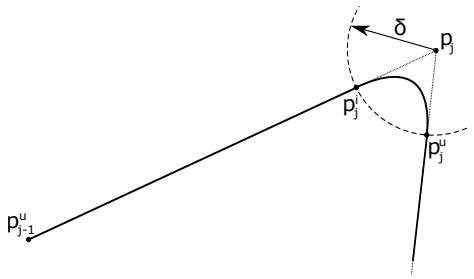

Figure 1: Control Points

with parabolas to obtain a smooth path. The parabolic trajectories are geometrically defined through points $\mathbf{p}_j^i$ and $\mathbf{p}_j^u$ which states the input and output of the trajectory. They are obtained using construction lines intersected with circles with δ radius centred on the vertices defined by $\mathbf{p}_j$. The approach can be further generalized for a three-dimensional space intersecting the previous segments with spheres of radius δ centred in the vertices and select the intersection points. To link straight lines using parabolic trajectories leads to straight lines limited by points $\mathbf{p}_{j-1}^u$ and points $\mathbf{p}_j^i$ as it's easily understandable.

It's possible to evaluate the derivatives of eq. 8 respect to u using the formula 7.

Computing for straight and parabola lines $d\mathbf{b}/du$ and $d^2\mathbf{b}/du^2$ and exploiting equations 3, $\dot{u}(t)$ and $\ddot{u}(t)$ are obtained.

LA FRASE PRECEDENTE ANDREBBE SPIEGATA MEGLIO

In this way all instruments needed to evaluate temporal derivatives of a *Bézier curves* through the use of eq.3 are available. Respectively for **straight** and **parabolic lines**:

$$\dot{\tilde{\mathbf{b}}}(t) = \left(-\mathbf{p}_{j-1}^u + \mathbf{p}_j^e\right)\dot{u} \qquad \ddot{\tilde{\mathbf{b}}}(t) = \left(-\mathbf{p}_{j-1}^u + \mathbf{p}_j^e\right)\ddot{u} \tag{9}$$

$$\begin{aligned}\dot{\tilde{\mathbf{b}}}(t) &= -2\left(1-u\right)\dot{u}\mathbf{p}_j^e + \left[2\dot{u}\left(1-u\right) - 2u\dot{u}\right]\mathbf{p}_j + 2u\dot{u}\mathbf{p}_j^u \\ \ddot{\tilde{\mathbf{b}}}(t) &= \left[\dot{u}^2 - 2(1-u)\ddot{u}\right]\mathbf{p}_j^e + \left[2\ddot{u}(1-u) - 2\dot{u}^2 - 2u\ddot{u}\right]\mathbf{p}_j + \left(2\dot{u}^2 + 2u\ddot{u}\right)\mathbf{p}_j^u\end{aligned} \tag{10}$$

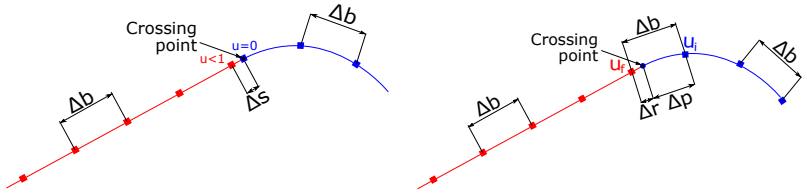

(a) Crossing point (b) Correction of the crossing point

Figure 2: Deposition trajectory

Now it is possible to evaluate the motion profile computing the $u(t)$ values in every instant considering the time discretization with sample time T_s. The goal is to generate a TVP[1] for parameter $u(t)$ in order to guarantee a constant material flow in all trajectory points. For part with constant acceleration eq.5 is used whereas for the central part of the path eq.4 is used. Pulling together straight and parabolic segments a velocity variation of the parametric variable is generated in the first point of the new segment when passing from the previous to the following. That's caused by the fact that in the crossing point the parametric value is not $u = 1$ but it's lower as shown by fig.2a. Since every segment is defined by a starting parametric value $u = 0$ a spatial distance is generated along the path $\Delta s < \Delta b$ between the last point of the straight line and the initial point of the parabolic line. It's necessary to attribute a suitable value of u to the first point of the parabolic line in order to obtain equally spaced points along the path, equal to Δb. Having as reference fig.2b, and being aware that $\Delta b = v_c \cdot T_s$ and $\Delta r = b_{line}(u = 1) - b_{line}(u_f)$ it's necessary to evaluate the right variable u_2 to collocate the first point of the parabolic line to a distance equal to Δb along the curve evaluated as $\Delta p = \Delta b - \Delta r$.

Rewriting conveniently equation 4 for the parabolic trajectory u_i is obtained

[1] trapezoidal velocity profile

according to the following expression:

$$u_i = \frac{\Delta p}{\left|\frac{d\mathbf{b}}{du}\right|_{u=0}} - \frac{\Delta p^2}{2}\left[\frac{\frac{d\mathbf{b}^T}{du}\cdot\frac{d^2\mathbf{b}}{du^2}}{\left|\frac{d\mathbf{b}}{du}\right|^4}\right]_{u=0} \tag{11}$$

The same procedure with the same rules is used for the crossing points between a parabola and a straight line. It's possible to evaluate $\Delta r = \Delta b - \Delta p$ where $\Delta b = v_c \cdot T_s$ whereas for the evaluation of Δb it is necessary to recall eq.4 replacing $u_{k+1} = 1$, $u_k = u_f$ and $v_c \cdot T_s = \Delta p$.

Operating the described substitutions, the following equation of second degree for the variable Δp is obtained:

$$\frac{1}{2}\left[\frac{\frac{d\mathbf{b}^T}{du}\cdot\frac{d^2\mathbf{b}}{du^2}}{\left|\frac{d\mathbf{b}}{du}\right|^4}\right]_{u_f}\Delta p^2 - \frac{1}{\left|\frac{d\mathbf{b}}{du}\right|_{u_f}}\Delta p + 1 - u_f = 0 \tag{12}$$

Solving with respect to Δp allows to calculate u_i on the straight line replacing it in the equation 4:

$$u_i = \frac{\Delta r}{\left|\frac{d\mathbf{b}}{du}\right|_{u=0}} \tag{13}$$

4.1. Example

INSERIRE UN PICCOLO ESEMPIO PER IL CALCOLO DI UNA TRAIETTORIA

A simple example is provided to demonstrate the use of the proposed approach. Let's consider the points .....

INSERIRE UN GRAFICO DEI PUNTI, IL GRAFICO DELLA TRAIETTORIA CON LE CURVE DI BEZIER

INSERIRE IL GRAFICO DELLA VELOCITA' DIMOSTRARE CHE L'APPROCCIO FORNISCE UNA OTTIMA APPROSSIMAZIONE, OVVERO, CHE LA VELOCITA' RIMANE ALL'INTERNO DI UN RANGE TRASCURABILE

5. Path planning with relaxed constant velocity constraint using Rational Bézier Curves

The path planning approach described in Section 4 can be further extended to improve the interpolation of the ideal trajectory, at the cost of a higher complexity of the calculations. This could be relevant in the cases where a higher accuracy is required and/or where different levels of accuracy are required in different points of the trajectory. Notice that, a better interpolation could also entails the need of relaxing the constraint on the constant velocity allowing a fluctuation in a given range, to take into consideration the dynamical behaviour and associated impact on the actuators of the robot. In this section we present an extension of the interpolation approach in Section 4 taking advantage of *Rational Bézier Curve*, i.e., a curve in $\mathbb{R}$ with $d = 2, 3$, being the projection of a polynomial Bézier curve in $\mathbb{R}^{d+1}$.

Given a set of control points $\mathbf{p}_j \in \mathbb{R}$ and a set of weights $w_j \in \mathbb{R}$ with $w_j \geq 0$, a *Rational Bézier Curves*, defined over the interval $[0, 1]$, can be written as:

$$\mathbf{R}(u) = \frac{\sum_{j=0}^{m} B_j^m(u) \cdot w_j \cdot \mathbf{p}_j}{\sum_{j=0}^{m} B_j^m(u) \cdot w_j} \tag{14}$$

If $w_j = 1 \forall j$, the rational Bézier curve is equal to a polynomial Bézier curve. Increasing the weight w_j pulls the curve to the control point $[p]_j$ while decreasing the weight $w - j$ pushes the curve away from it (Figure 3). In the limit case, when $w_j \to \infty$, the interpolation curve tends to the piecewise linear sequence of segments joining the points.

In a similar way, the results related to the differentiation of Rational Bézier Curves could be exploited [20]. The derivative of a rational bézier curve in its general form is:

$$\mathbf{P}^{'}(u) = \sum_{j=0}^{m-1} \lambda_j(u)(\mathbf{P}_{j+1} - \mathbf{P}_i) \tag{15}$$

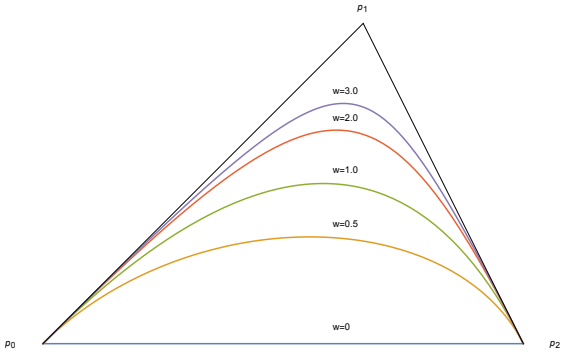

Figure 3: Rational Bézier Curves with different w.

where, for $j = 0, \ldots, m-1$,

$$\lambda_j(u) = \frac{1}{(1-u)uw_{0,m}^2(u)} \sum_{i=0}^{j} \sum_{k=j+1}^{m} (k-i) B_{j,m}(u) B_{k,m}(u) w_i w_k \tag{16}$$

where $B_{i,m}(u)$ are the Bernstein polynomials and the weights $w_{i,k}(u)$ are defined as:

$$\sum_{j=0}^{k} B_{j,k}(u) w_{i+j} \tag{17}$$

Let us consider a quadratic curve defined by three points:

$$\mathbf{P}(u) = \frac{(1-u)^2 \mathbf{p}_1 + 2wu(1-u)\mathbf{p}_2 + u^2 \mathbf{p}_3}{(1-u)^2 + 2wu(1-u) + u^2} \tag{18}$$

$$\begin{aligned}
\lambda_0(u) &= \frac{1}{(1-u)uw_{0,2}^2(u)} \sum_{j=0}^{0} \sum_{k=1}^{2} k B_{j,2}(u) B_{k,2}(u) w_j w_k = \\
&= \frac{1}{(1-u)uw_{0,2}^2(u)} [1 B_{0,2}(u) B_{1,2}(u) w_0 w_1 + 2 B_{0,2}(u) B_{2,2}(u) w_0 w_2] = \\
&= \frac{1}{(1-u)uw_{0,2}^2(u)} [(1-u)^2 2u(1-u) w_0 w_1 + 2(1-u)^2 u^2 w_0 w_2]
\end{aligned} \tag{19}$$

$$\lambda_1(u) = \frac{1}{(1-u)uw_{0,2}^2(u)} \sum_{j=0}^{1}\sum_{k=2}^{2}(k-j)B_{j,2}(u)B_{k,2}(u)w_j w_k =$$
$$= \frac{1}{(1-u)uw_{0,2}^2(u)}[2B_{0,2}(u)B_{2,2}(u)w_0 w_2 + B_{1,2}(u)B_{2,2}(u)w_1 w_2] =$$
$$= \frac{1}{(1-u)uw_{0,2}^2(u)}[2(1-u)^2u^2w_0w_2 + 2u(1-u)u^2w_0w_2] \tag{20}$$

where,

$$w_{0,2}(u) = \sum_{j=0}^{2} B_{j,2}(u)w_j = B_{0,2}(u)w_0 + B_{1,2}(u)w_1, B_{2,2}(u)w_2 =$$
$$= (1-u)^2w_0 + 2u(1-u)w_1 + u^2w_2 \tag{21}$$

To obtain the first derivative of the rational Bézier curve, the expressions of $\lambda_0(u)$ and $\lambda_1(u)$ must be substituted in:

$$\mathbf{P}^{'}(u) = \lambda_0(u)(\mathbf{p}_1 - \mathbf{p}_0) + \lambda_1(u)(\mathbf{p}_2 - \mathbf{p}_1) \tag{22}$$

The expression of the second derivative is more complex [20]:

$$\mathbf{P}^{''}(u) = m\frac{w_{2,m-2}(u)}{w_{0,m}^3(u)}(2mw_{0,m-1}^2 - (m-1)w_{0,m-2}w_{0,m} - 2w_{0,m-1}w_{0,m})(P_{2,m-2}(u) - P_{1,m-2}(u))$$
$$- m\frac{w_{0,m-2}(u)}{w_{0,m}^3(u)}(2mw_{1,m-1}^2(u) - (m-1)w_{2,m-1}w_{0,m} - 2w_{1,m-1}w_{0,m})(P_{1,m-2}(u) - P_{0,m-2}(u)) \tag{23}$$

where

$$\mathbf{P}_{i,k}(u) = \frac{\sum_{j=0}^{k} B_{j,k}(u)w_{i+j}\mathbf{p}_{i+j}}{\sum_{j=0}^{k} B_{j,k}(u)w_{i+j}} \tag{24}$$

The approach described in Section 4 can be applied using these expression for the calculation of $\dot{u}(t)$ and $\ddot{u}(t)$ to calculate the values of $u(t)$ according to the discretization adopted. The use of different weights can allow different degrees of accuracy along the trajectory.

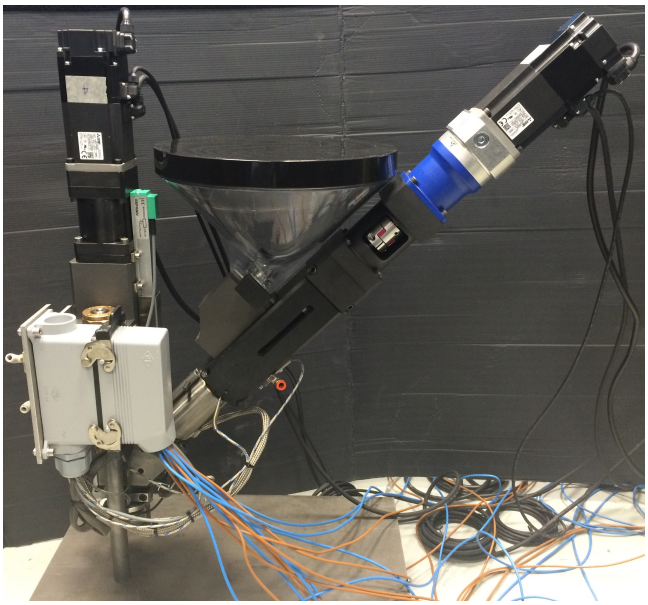

Figure 4: Extrusion system

6. Application to an additive manufacturing machine prototype

As described in the introduction, the proposed approach grounds on research activities carried out Politecnico di Milano related to an innovative additive manufacturing process and equipment [5]. The process is based on a metal injection molding (MIM) extruder shown in Fig.4. A feedstock of metal powder and polymeric binder is poured in the right side of the machine where is heated and pressed in a downstream chamber from wherein it is extruded. The so called *green body* obtained is then sintered to obtain the final object. This process is a potential alternative to additive manufacturing techniques for metal printing, where usually laser or electron based melting techiques are used and whose costs is rather high. In Fig.4 it also possible to see the two electrical motors controlling the extrusion system. One motor pushes the feedstock in the final chamber where the material is extruded through a piston controlled by the other motor. Controlling the extrusion motor is the main drive to control the process and, hence, the extrusion rate. Due to the preliminary phase of the

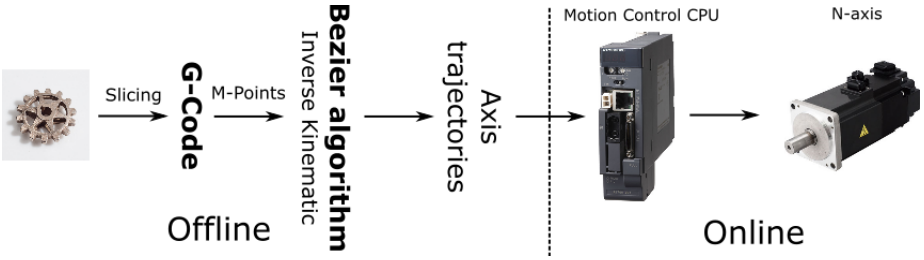

Figure 5: Path algorithm implementation

process development and the difficulty to characterize and operated the process in a wide range of the technological parameters, the extrusion head is operated with a constant extrusion rate. Hence, the path planning approach described in Section 4 is used.

Ho inserito la frase precedente per giustificare l'utilizzo di velocita costante nella parte sperimentale, oltre che giustificare tecnologicamente l'approccio

The described extrusion system is mounted on a machine structure based on a linear delta robot, where a mobile platform is moved to operate the obtained path. The parametric velocity associated to the movement of the platform is calibrated together with the extrusion rate of the devices in Fig.4.

Differently from traditional cartesian CNC machines, the trajectory of the extrusion head must be further processed through the inverse kinematic equations associated to the machine architecture, deriving the trajectories for the actuators. In the current version of the machine prototype, these steps are operated off-line. A motion control CPU together with servo systems closes the control loops for each actuator.

6.1. Machine Design

The prototype of the machine described in the previous Section is shown in Fig.6 [4]. The picture on the left shows the delta robot architecture capable to translate the platform where the extruded material is laid down. The picture on the right shows the control system based on PLCs and a module for the control of the three motion axes and the two motors of the extruder.

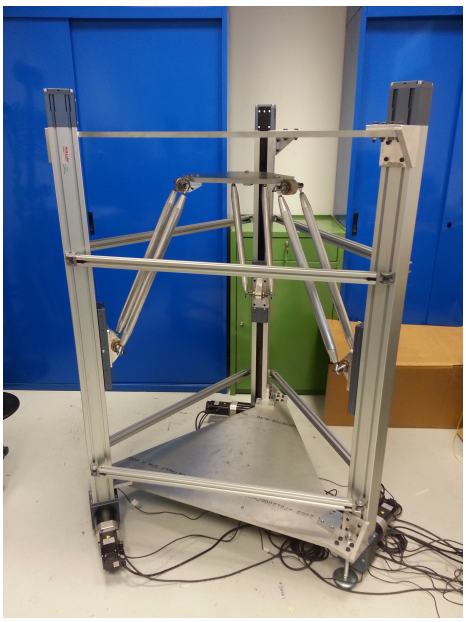

(a) Linear Delta

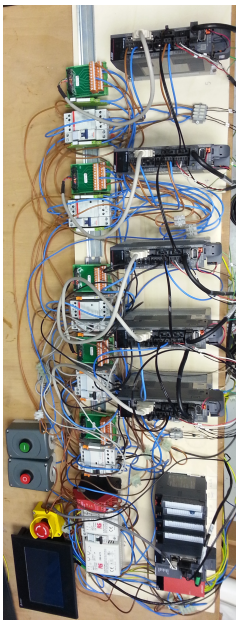

(b) Control System

Figure 6

The linear delta moves the platform in accordance with the extrusion rate of the extruder which is going to be installed on the top of the machine (Fig.7a). The three axis managed by the motion control module correspond to the displacement of three sliders along the three linear guides visible in Fig.6a. The motion module also controls the extruder through its two motors and keep velocity of the motor driving the extrusion rate constant to guarantee a constant material deposition in time, jointly controlling the parametric velocity of the platform following the desired trajectory.

6.2. Testing

The trajectory defined through the proposed algorithm has bee first tested through a dynamic simulation model of the system created using the Adams®software7b. This environment provides the capability of estimating the torques and accelerations of the motors, given a path to be executed. The analysis of the results

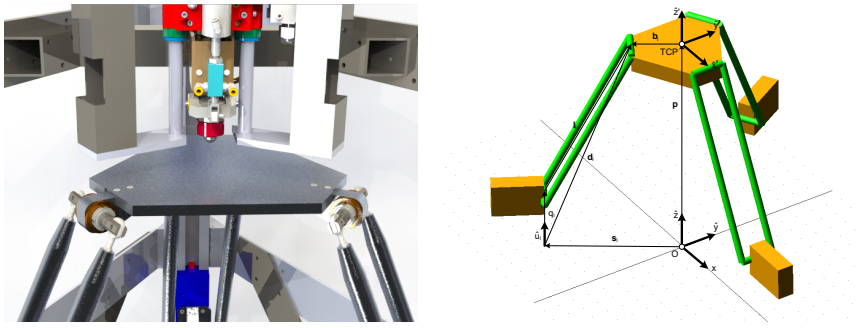

(a) AM machine (b) Dynamic Model

Figure 7

clearly show that a constant parametric velocity in the trajectory (and, hence, of the platform) causes acceleration peaks of the motors. Moreover, small fluctuations of the platform velocity cannot be avoided due to the complexity of the machine architecture. Nevertheless, for this AM application, the magnitude of these fluctuations is negligible.

In addition, the proposed path planning algorithm has been used to derive an exemplary path to be tested on the machine prototype.

To decouple the performance of the path planning approach from the characteristics of the extruder, a red pen has been used as end effector to draw the movements of the platform on the paper (Fig.8a). The path obtained is shown in Fig.8b.

It is worth to compare the parametric velocity $\dot{u}$ of the platform and the accelerations obtained on the active joints of the machine. In Fig.9b, the blue circle represents the desired path for the platform. It has been evaluated starting from $\mathbf{p}_j$ points obtained intersecting a circle with straight lines and, hence, simulating the results of a slicing procedure. Hence, the interpolation has been used to evaluate the platform trajectory. The red circle, matching almost perfectly the blue one, is the real platform trajectory, evaluated measuring the position of the motors through their encoders and using the direct kinemat-

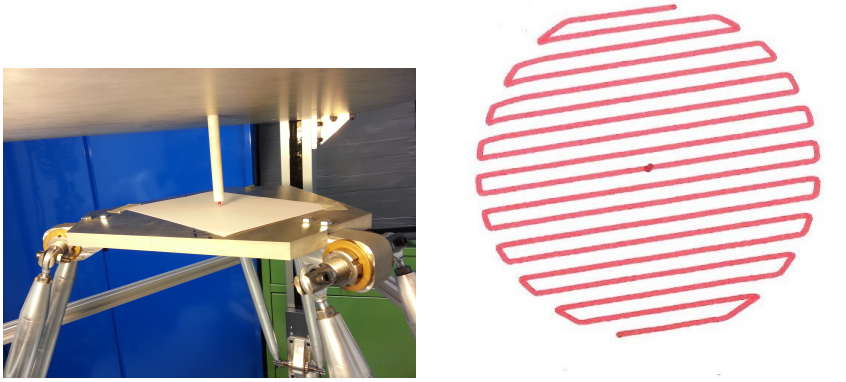

(a) Deposition System (b) Drawing

Figure 8: Deposition application

ics equations. The implementation of the system on an industrial architecture leads to small position errors during the movements. The parametric velocity $\dot{u}$ has been set to $5[mm/s]$ and a fillet radius $\delta = 0.45[mm]$ has been chosen. No weight has been used in this example by not having points more important than others along the trajectory. Looking at Fig.9a, it is interesting to notice how, even with a constant parametric velocity, acceleration peaks affects the motors, whose entity could possibly be infeasible. Actually, constant parametric velocity along the deposition path leads to high accelerations in the curves. Looking the details, it can be seen how acceleration peaks appear in correspondence with the inversion of the direction of axis 3, which corresponds to the curves of the path reported in Fig.9b.

The change of direction of the axis, its corresponding acceleration peak and the trajectory curve of the platform are highlighted with red circles. The acceleration peaks lead to small velocity fluctuations along the path of the linear delta platform as expected.

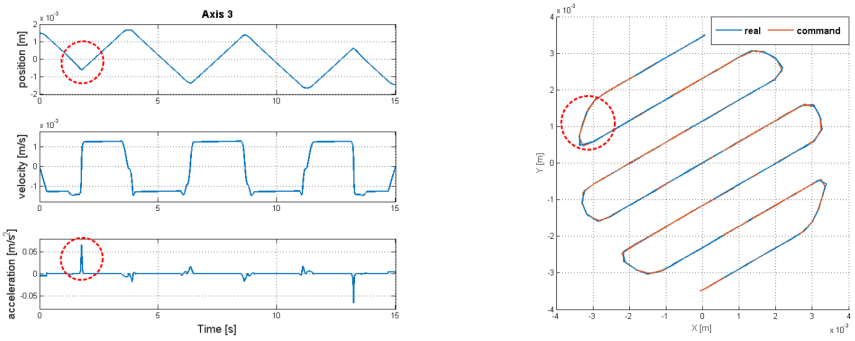

(a) axis 3 (b) Platform trajectory

Figure 9

7. Conclusions

In this paper we presented and tested a path planning algorithm to control the material deposition rate in accordance with a TCP trajectory during the execution of an industrial process. The motivation to this research grounds on the need to operate a novel additive manufacturing process in a machine prototype.

The use of this approach has been demonstrated in a real additive manufacturing application with a linear delta robot controlled by an industrial PLC and a motion control unit. Moreover, the use of an industrial control system allows to show the possibility to adopt this solution in real industrial applications.

In addition, the application to a peculiar machine architecture has shown how the need to transform the path generated by the algorithm into trajectories for the axes could entail acceleration peaks that must be kept at bay to avoid high stress for the actuators and induced vibration in the process.

Future research will address experiments with the real extrusion device as well as the possibility of taking advantage of controlling the extrusion rate in order to both increase the accuracy of the interpolation and reduced the stress on the actuators.

Bibliography

[1] I. Stratasys, modeling apparatus for three-dimensional objects, US Patent 5340433.

[2] D.Roberson, C.M.Shemelya, E.MacDonald, R.Wicker, Expanding the applicability of fdm-type technologies through materials development, Rapid Prototyping Journal 21 (2015) 137 – 143.

[3] N.Volpato, D.Kretschek, J.A.Foggiatto, C. da Silva Cruz, Experimental analysis of an extrusion system for additive manufacturing based on polymer pellets, International Journal of Advanced Manufacturing Technology 81 (2015) 1519–1531.

[4] E.Fiore, H.Giberti, L.Sbaglia, Dimensional synthesis of a 5-dof parallel kinematic manipulator for a 3d printer, in: 16th International Conference on Research and Education in Mechatronics REM, 2015.

[5] H.Giberti, M. Strano, M. Annoni, An innovative machine for fused deposition modeling of metals and advanced ceramics, in: MATEC Web of Conferences, 2016.

[6] H.Giberti, E.Fiore, L.Sbaglia, Kinematic synthesis of a new 3d printing solution, in: MATEC Web of Conferences, 2016.

[7] O.A.Mohamed, S.H.Masood, J.L.Bhowmik, Optimization of fused deposition modeling process parameters for dimensional accuracy using i-optimality criterion, Measurement 81 (2016) 174–196.

[8] A.Boschetto, V.Giordano, F.Veniali, Modelling micro geometrical profiles in fused deposition process, International Journal of Advanced Manufacturing Technology 61 (2012) 945–956.

[9] Y.Jin, J.Zhang, Y.Wang, Z.Zhu, Filament geometrical model and nozzle trajectory analysis in the fused deposition modeling process, Journal of Zhejiang University SCIENCE A.

[10] K. Jiang, Y. Gu, Controlling parameters for polymer melting and extrusion in fdm, Key Engineering Materials.

[11] P. Kulkarni, D. Dutta, Deposition strategies and resulting part stiffnesses in fused deposition modeling, Journal of Manufacturing Science and Engineering.

[12] G. Jin, W. Li, C. Tsai, L. Wang, Adaptive tool-path generation of rapid prototyping for complex product models, Journal of Manufacturing Systems.

[13] G. Jin, W. Li, L.Gao, An adaptive process planning approach of rapid prototyping and manufacturing, Robotics and Computer-IntegratedManufacturing.

[14] J. Mireles, D. Espalin, D. Roberson, B. Zinniel, F. Medina, R. Wicker, Fused deposition modeling of metals, 23rd Annual International Solid Freeform Fabrication Symposium - An Additive Manufacturing Conference.

[15] O. RISHI, Feed rate effects in freeform filament extrusion (2012/2013).

[16] B.Thompson, H.S.Yoon, Efficient path planning algorithm for additive manufacturing systems, IEEE Transactions on Components, Packaging and Manufacturing Technology 4 (2014) 1555–1563.

[17] Y.A.Jin, Y.He, J. W. Z. Lin, Optimization of tool-path generation for material extrusion-based additive manufacturing technology, Additive Manufacturing 1 (2014) 32–47.

[18] B.Sencer, K.Ishizaki, E.Shamoto, A curvature optimal sharp corner smoothing algorithm for high-speed feed motion generation of nc systems along linear tool paths, Int.J. of Advanced Manufacturing Technology 76 (2015) 1977–1992.

[19] L. Biagiotti, C. Melchiorri, Trajectory planning for automatic machines and robots, Springer Berlin Heidelberg.

[20] S. Floater, Derivatives of rational bézier curves, Computer Aided Geometric Design 9 (1992) 161–174.